โครงการ

การเรียนการสอนเพื่อเสริมประสบการณ์

ชื่อโครงการ การดูดซับและการเปลี่ยนแก๊สขนาดเล็กบนผิวของเบอริลเลียมออกไซด์

Adsorption and interaction of small gases on the BeO

ชื่อนิสิต นายพัสกร เปียระบุตร

ภาควิชา เคมี

ปีการศึกษา 2558

คณะวิทยาศาสตร์ จุฬาลงกรณ์มหาวิทยาลัย

การดูดซับและการเปลี่ยนแก๊สขนาดเล็กบนผิวของเบอริลเลียมออกไซด์

Adsorption and interaction of small gases on the BeO

โดย
นายพัสกร เปียระบุตร

รายงานนี้เป็นส่วนหนึ่งของการศึกษาตามหลักสูตร
ปริญญาวิทยาศาสตรบัณฑิต
ภาควิชาเคมี คณะวิทยาศาสตร์
จุฬาลงกรณ์มหาวิทยาลัย
ปีการศึกษา 2558

Project Title: Adsorption and interaction of small gases on the BeO

Student name: Mr. Pasakorn Piarabutr

Field of study: Chemistry

Project Advisor: Professor Dr. Vithaya Ruangpornvisuti

Accepted by Department of Chemistry, Faculty of Science, Chulalongkorn University in Partial Fulfillment of the Requirements for the Degree of Bachelor of Science.

……………………………………….Head of Department of Chemistry

(Associate Professor Dr. Vudhichai Parasuk)

PROJECT COMMITTEE

……………………………………….Chair committee

(Professor Dr. Tirayut Vilaivan)

……………………………………….Project Advisor

(Professor Dr. Vithaya Ruangpornvisuti)

……………………………………….Committee

(Associate Professor Chuchaat Thammacharoen)

Writing quality of this report is: ☐ Very good   ☐ Good   ☐ Pass

ชื่อโครงการ　　　　　การดูดซับและการเปลี่ยนแก๊สขนาดเล็กบนผิวของเบอริลเลียมออกไซด์

ชื่อนิสิตในโครงการ　　　นายพัสกร　　เปียระบุตร　　　　เลขประจำตัว　5533124523

ชื่ออาจารย์ที่ปรึกษา　　　ศ.ดร.วิทยา　　เรืองพรวิสุทธิ์

ภาควิชาเคมี คณะวิทยาศาสตร์ จุฬาลงกรณ์มหาวิทยาลัย ปีการศึกษา 2558

บทคัดย่อ

　　　　ในงานวิจัยนี้ได้ศึกษาการดูดซับโมเลกุลแก๊สขนาดเล็กได้แก่ แก๊สไฮโดรเจน ไนโตรเจน ออกซิเจน คาร์บอนมอนออกไซด์ ไนโตรเจนมอนออกไซด์ น้ำ ไนโตรเจนไดออกไซด์ แอมโมเนีย ซัลเฟอร์ไดออกไซด์ คาร์บอนไดออกไซด์ ไนตรัสออกไซด์บนเบอริลเลียมออกไซด์ที่มีโครงสร้างลักษณะคล้ายกรงโซดาไลท์ (BeOSL:$Be_{12}O_{12}$) โดยการคำนวณด้วยวิธี DFT/B3LYP/6-31+G(d,p) พบว่าการดูดซับของไนโตรเจนไดออกไซด์ที่หันไนโตรเจนมาทางด้านบนของเบอริลออกไซด์โซดาไลท์มีค่าพลังงานการดูดซับมากที่สุด โดยมีค่าเท่ากับ -39.54 กิโลแคลอรี่ต่อโมล ค่าการเปลี่ยนแปลงช่องว่างระดับพลังงานของเบอริลเลียมออกไซด์โซดาไลท์หลังจากดูดซับกับไนโตรเจนไดออกไซด์และออกซิเจนมีค่าลดลง -71.77% และ -32.85 % เมื่อเปรียบเทียบกับโครงสร้างก่อนการดูดซับ ตามลำดับ ดังนั้นเบอริลเลียมออกไซด์โซดาไลท์อาจสามารถนำไปเป็นวัสดุรับรู้ก๊าซไนโตรเจนไดออกไซด์และออกซิเจนได้ และผลจากการคำนวณการเป็นตัวเร่งปฏิกิริยาของเบอริลเลียมออกไซด์โซดาไลท์ในปฏิกิริยาออกซิเดชันของคาร์บอนมอนออกไซด์โดยแก๊สไนตรัสออกไซด์เพื่อให้ได้ผลิตภัณฑ์เป็นแก๊สที่ไม่มีพิษคือคาร์บอนไดออกไซด์และไนโตรเจนโดยมีค่าพลังงานกระตุ้นเท่ากับ 46.14 กิโลแคลอรี่ต่อโมลและได้เสนอแนะกลไกการเกิดของปฏิกิริยานี้

คำสำคัญ : การดูดซับ, แก๊ส, เบอริลเลียมออกไซด์

Title:	Adsorption and interaction of small gases on the BeO
Student name:	Mr. Pasakorn Piarabutr	ID: 5533124523
Advisor name:	Professor Dr. Vithaya Ruangpornvisuti

Department of Chemistry, Faculty of Science, Chulalongkorn University, Academic Year 2015

Abstract

In this study, adsorptions of diatomic (H_2, N_2, O_2, CO, NO), triatomic (CO_2, N_2O, NO_2, H_2O, SO_2) and tetratomic (NH_3) gases on the BeO sodalite−like cage ($Be_{12}O_{12}$) were studied using the DFT/B3LYP/6−31+G(d,p) method. Nitrogen dioxide adsorption by pointing its nitrogen atom toward Be atom of the BeOSL cluster was found to be the most favorable process. The adsorption energy for nitrogen dioxide is −39.54 kcal/mol which is much stronger than other studied gases. Changes of energy gaps of adsorption structures of NO_2 (ΔE_g= −71.77%) and O_2 (ΔE_g=−32.85%) on the BeOSL compared with clean BeOSL may suggest that the BeOSL cluster can be used as the sensing material for NO_2 and O_2. As a test of the BeOSL as catalyst for CO reacting with N_2O to afford CO_2 and N_2 non−toxic gases, its activation energy of 46.14 kcal/mol was obtained and its mechanism was proposed.

Keyword: adsorption, DFT, gas, BeO

ACKNOWLEDGEMENTS

CONTENTS

LIST OF FIGURES

LIST OF TABLES

CHAPTER I

INTRODUCTION

1.1 Background and Literature review

BeO has been used in various applications such as nuclear fuel [1] hydrogen storage [2]. Gas adsorption is one of the most study issue in many scientific areas [3−9]. Nevertheless, there is a few study of small molecule adsorption on BeO. Peyghan et al [10] studied on adsorption of CO_2 molecule in the interior and exterior surface of a BeO nanotube (BeONT). The result indicated that increasing the number of adsorbed CO_2 molecule, the adsorption energy is decreased, It was found that the energy gap of BeONT is not sensitive to the presence CO_2 molecule due to its value is slightly changed. Rastegar et al [11] investigated the adsorption of COH_2 molecule on BeONT. It was found that their energy gaps have been decreased significantly. The BeONT used as a potential and effective gas sensor for COH_2 detection. Ahmadaughaei et al [12] studied adsorption of H_2S on the pristine and Si−doped BeONT. It was found that H_2S molecule is physically adsorbed on pristine BeONT and interaction of Si_O−BeONT with H_2S molecule is energetically more favorable than pristine BeONT and Si_{Be}−BeONT. The largely change of energy gap suggested that Si−doped tube might be sensitive to the H_2S molecule. Barzilai et al [13] investigated the adsorption of Au on a hexagonal BeO (0001) wurtzite structure. The calculations showed that the most favorable adsorption site for Be−terminated surface is located above the Be−Be bridge bond and O−terminated surface it located above O.

Many previous studies, BeO structures existed as is nanotubes were mostly taken [14−15]. Ren et al [16] studied structures of $(BeO)_n$ ($n = 2$−12, 16, 20 and 24) cluster using the method combining the genetic algorithm with density functional theory. It showed that the global minimum structures of $(BeO)_n$ cluster are in cage form when $n \geq 8$. The adsorption gas on BeO sodalite structure has not been investigated.

Hwang et al [17] investigated reaction mechanism in the BeO/CO/H$_2$ system. Adsorption abilities on cluster surface can be used in the redox reaction. The results indicated that there are two pathways of mechanism the first and second pathway are: BeO+CO+H$_2$ → OBeOC+H$_2$ → OBeOCH$_2$ → BeO+H$_2$CO, and BeO+CO+H$_2$→ HBeOH+CO → t−HCOBeOH → OBeOCH$_2$ → BeO+H$_2$CO, respectively.

1.2 Theoretical background

Quantum chemical calculations consist of two main methods, semi−empirical and Ab−initio methods. Ab−initio method is categorized as Hartree−Fock (HF) and density functional theory (DFT) methods. These methods are used to explain and predict on chemical behavior. Ground state of individual atom and molecule, excited state, transition state that occur during the chemical reaction are related to the quantum mechanical [18].

1.2.1 Ab Initio method

Ab initio calculations is a method based on quantum chemistry [19]. This method is significantly participated with Schrödinger equation, equation (1.1)

$$-\frac{\hbar^2}{2m}\nabla^2\Psi(r,t) + V(r)\Psi(r,t) = i\hbar\frac{\partial\Psi(r,t)}{\partial t} \quad (1.1)$$

when $\hbar = h/2\pi$ and h is Planck's constant, m is mass of particle. ∇^2 is the Laplacian operator, which in Cartesian coordinates is given by $\nabla^2 = \frac{\partial^2}{\partial x^2} + \frac{\partial^2}{\partial y^2} + \frac{\partial^2}{\partial z^2}$. $V(r)$ is the potential energy function which returns the potential energy of the particle as a function of its position within the field.

The same time− and position− independent constant of both side is required to satisfy this equation. The constant become a possible energy of the particle, which is the reason for setting the left hand side of this equation equal to the constant, after rearrangement of some term, yields in equation (1.2)

$$-\frac{\hbar^2}{2m}\nabla^2\Psi(r) + V(r)\Psi(r) = E\Psi(r) \quad (1.2)$$

This particular equation is called the time–independent Schrodinger equation. It gives the part of the Schrodinger equation that depends only on position. It is common to rewrite the left hand side as an operator called the Hamiltonian, H, such that

$$\Psi(r) = E\Psi(r)$$

$$\text{where } H = -\frac{\hbar^2}{2m}\nabla^2 + V(r) \tag{1.3}$$

An operator is simply conversion of one function to another function. Quantum mechanics makes extensive use of operators, as all observables (like energy, momentum, velocity, etc) are formulated as operators.

$$\widehat{H}\Psi = E\Psi \tag{1.4}$$

Where $\widehat{H}$ is Hamiltonian operator, E is the total energy of the system and Ψ is the n–electron wave function, respectively.

$$\widehat{H} = -\frac{\hbar^2}{2m_e}\sum_i^{electrons}\nabla_i^2 - \frac{\hbar^2}{2}\sum_A^{nuclei}\frac{1}{M_A}\nabla_A^2 - \frac{e^2}{4\pi\varepsilon_0}\sum_i^{electron}\sum_A^{nuclei}\frac{Z_A}{r_{iA}}$$

$$+ \frac{e^2}{4\pi\varepsilon_0}\sum_i^{electrons}\sum_j^{electrons}\frac{1}{r_{ij}} + \frac{e^2}{4\pi\varepsilon_0}\sum_A^{nuclei}\sum_B^{nuclei}\frac{Z_A Z_B}{R_{AB}} \tag{1.5}$$

Where Z is the nuclear charge, M_A is the mass of electron, R_{AB} is the distance between nuclei A and B, r_{ij} is the distance between electrons i and j, r_{iA} is the distance between electron i and nucleus, and ε_0 is the permittivity of free space.

1.2.2 Density functional theory DFT method

DFT is a computational quantum mechanical modelling method used in physics, chemistry and materials science to investigate the electronic structure of many−body systems. The properties of a many−electron system can be determined by using by electron density (ρ) that was later confirmed by Hohenberg and Kohn in 1964. DFT method became very popular in quantum chemistry due to its can approximate functionals to provide a useful balance between accuracy and computational cost [20]. This allowed to have an efficiency accuracy of calculation even if in larger system. Conventional wavefunction methods, either variational or perturbative, can be applied to find highly accurate results smaller systems, providing benchmarks for developing density functionals, which can then applied to much larger system.

1.2.2.1 Kohn-Sham equations

To provide a DFT method effectively without losing an accuracy, Kohn and Sham method was used to solve the problem of the system of interacting electrons onto a fictitious system of non−interacting electrons [20-21]. The variational problem for the Hohenberg−Kohn density−functional was described down below, introducing a Lagrange multiplier μ to constrain the number of electrons to be *N:*

$$\delta[F(N) + \int dr\, V_{ext}(r)n(r) - \mu(\int dr\, n(r) - N)] = 0 \tag{1.6}$$

Kohn and Sham separated *F(N)* into three parts

$$F(N) = T_s(n) + \frac{1}{2}\int dr\, dŕ\, \frac{n(r)n(ŕ)}{|r-ŕ|} + E_{xc}(n) \tag{1.7}$$

Which $T_s(n)$ is referred to the kinetic energy of a non−interacting gas with density *n(r)*. The second term is the classical electrostatic (Hartree) energy and the final term is an implicit definition of the exchange−correlation energy which contains the non−classical electrostatic interaction energy and the difference between the kinetic energies of the interacting and non− interacting systems. This calculation can be divided into two terms. First two terms are simple to understand. Last term is a small fraction of the total energy which contains the effects of

the complex behavior. This term can be approximated surprisingly well. Using this separation, equation (1.6) can be rewritten:

$$\frac{\delta T_S(n)}{\delta n(r)} + V_{ks}(r) = \mu \tag{1.8}$$

The Kohn–Sham potential $V_{ks}(r)$ is given by

$$V_{ks}(r) = \int d\acute{r} \frac{n(\acute{r})}{|r-\acute{r}|} + V_{xc}(r) + V_{ext}(r) \tag{1.9}$$

And the exchange–correlation potential $V_{xc}(r)$ is

$$V_{xc}(r) = \frac{\delta E_{xc}(n)}{\delta n(r)} \tag{1.10}$$

In order to find the ground–state density $n_0(r)$ for this non–interacting system. Simply solve the one–electron Schrödinger equations is required;

$$[(-\frac{1}{2}\nabla^2 + V_{KS}(r)]\Psi_i(r) = \varepsilon_r \Psi_i(r) \tag{1.11}$$

For $\frac{1}{2}N$ single–particle $|\Psi_i\rangle$ with energies, ε_i constructing the density from

$$n(r) = 2\sum_{i=1}^{\frac{n}{2}} |\Psi_i(r)|^2 \tag{1.12}$$

Assume that orbitals are singly–occupied. Add of factor 2 is necessary for spin degeneracy and the non-interacting kinetic energy $T_s(n)$ from

$$T_s(n) = -\sum_{i=1}^{\frac{n}{2}} \int dr \Psi_i^*(r)\nabla^2\Psi_i(r) \tag{1.13}$$

It is necessary to solve these equations self–consistently. Since $V_{KS}(r)$ the Kohn–Sham potential depends upon the density. Set of orbitals $\Psi_i(r)$ from a newly constructed density is obtained from solving The Schrödinger equation. The process repeated until the input and output densities are the same.

The energy of the non–interacting system, the sum of one–electron eigenvalues, is

$$2\sum_{i=1}^{\frac{n}{2}} \varepsilon_i = T_s(n) + \int dr\, V_{KS}(r)n(r)$$

$$= T_s(n) + \int dr\, d\acute{r}\, \frac{n(r)n(\acute{r})}{|r-\acute{r}|} + \int dr\, V_{xc}(r)n(r) + \int dr\, V_{ext}(r)n(r) \quad (1.14)$$

Compared to the interacting system, there are double–counts the Hartree energy and over–counts the exchange–correlation energy so the actually interacting energy is

$$E = 2\sum_{i=1}^{\frac{N}{2}} \varepsilon_i - \frac{1}{2}\int dr\, d\acute{r}\, \frac{n(r)n(\acute{r})}{|r-\acute{r}|} - \int dr\, V_{xc}(r)n(r)$$

$$+ \int dr\, n(r)V_{xc}(r) + E_{xc}(n) \quad (1.15)$$

To solve the Schrödinger equation for the extended non–interacting orbitals $\Psi_i(r)$ directly, a computational effort which scales as the cube of the system–size N is required, due to the cost of diagonalising the Hamiltonian or orthogonalising the orbitals, whereas the original complexity of finding a minimum of the Hohenberg–Kohn functional only required an effort which scaled linearly with N. The Kohn–Sham scheme need to be modified by a linear scaling method.

1.2.2.2 Hybrid methods

Hybrid functionals are improved approximations to the exchange and correlation (XC) energy component of the total energy of a system of electrons [22]. Hybrid function is different from standalone method since the standard density functionals (LDA and GGA) give a total energy from the only electronic density while the hybrid functionals method give a result from electronic density and the individual electronic wavefunctions. The exchange part of the XC energy is computed more or less exactly from the electron wave functions and mixed into the LDA or GGA energy.

One of the most popular hybrid functional B3LYP [27–28]. B3LYP is a combination of an exchange–energy functional invented by Becke and Steven that is the introduction of LYP correlation energy. Accordingly this correlation functional called B3LYP functional is as follow:

$$E_{XC}^{B3LYP} = (1 - a_0 - a_x)E_X^{LSDA} + a_0 E_X^{HF} + a_X E_X^{B88} + (1 - a_0)E_X^{VWN} + a_C E_C^{LYP} \quad (1.16)$$

where E_X^{LSDA} is the accurately pure DFT local spin–density approximation non–gradient–corrected exchange functional, E_X^{HF} is the Kohn–Sham orbitals based HF exchange energy functional, E_X^{B88} is the Becke 88 exchange functional

$$E_X^{B88} = E_X^{B88} + \Delta E_X^{B88} \; ;$$

$$\Delta E_X^{B88} = -\beta \rho^{1/3} \frac{x^2}{1 + 6\beta x \sinh^{-1} x} \quad (1.17)$$

The β parameter is determined by fitting to known atomic data and x is a dimension gradient variable. The E_X^{VWN} is the Vosko, Wilk, Nusair function (VWN) is given by

$$E_X^{VWN} = E_X^{LDA}(1 + ax^2 + bx^4 + cx^6)^{1/5}$$

$$x = \left| \frac{\nabla p}{\rho^{4/3}} \right| \quad (1.18)$$

1.2.3 Gaussian basis sets

A basis set is a mathematical description of the orbitals within a system used to perform the theoretical calculation [23–24]. Larger basis sets approximate more accurately the orbitals by imposing fewer restrictions on the locations of the electrons in space.

Linear combination of atomic orbitals (LCAO) was used to form the orbitals in Standard basis sets for electronic structure calculations. Basis sets assign a group of basis functions to each atom within a molecule to approximate its orbitals. These basis functions themselves are consisted of a linear combination of gaussian functions; such basis functions are referred to as contracted functions, and the component gaussian functions are referred to as primitives. A basis function consisting of a single gaussian function is termed uncontracted. However, the use of this function was not cost effective, and early numerical calculation were carried out using Slater–type orbitals (STOs).

$$\phi(r,\theta,\phi) = \frac{(2\zeta/a_0)^{n+1/2}}{[(2n)!]^{1/2}} r^{n-1} e^{-\zeta\, r/a_0} Y_l^m(\theta,\phi) \tag{1.19}$$

Further work showed that the cost of calculations can be further reduced if the AOs are expanded in terms of Gaussian functions, which have the form

$$g_{ijk}(r) = N x^i y^j z^k e^{-\alpha r^2} \tag{1.20}$$

1.2.3.1 Minimal basis sets

The smallest number of function called minimal basis sets. The most widely used of minimal basis set is STO–3G where a linear combination of three GTOs is fitted to an STO. The STO–nG basis set are available almost all element in the periodic table.

$$\phi(2s) \ = \ d_{1s}e^{-\alpha_{1s}r} + d_{1s}e^{-\alpha_{1s}r} + d_{1s}e^{-\alpha_{1s}r}$$

$$\phi\left(2p_x\right) = \ d_{1p_x}e^{-\alpha_{1p}r} + d_{2p_x}e^{-\alpha_{2p}r} + d_{3p_x}e^{-\alpha_{3p}r}$$

$$\phi\left(2p_x\right) = \ d_{1p_y}e^{-\alpha_{1p}r} + d_{2p_y}e^{-\alpha_{2p}r} + d_{3p_y}e^{-\alpha_{3p}r}$$

$$\phi\left(2p_x\right) = \ d_{1p_z}e^{-\alpha_{1p}r} + d_{2p_z}e^{-\alpha_{2p}r} + d_{3p_z}e^{-\alpha_{3p}r} \tag{1.21}$$

1.2.3.2 Split–valence basis sets

Split valence basis set is when the core electron and valance electron use the different basis set. Valence electron are more affected by chemical environment than the core electron, they are treated with a larger basis sets while the core electron are treated with minimal basis sets. For larger molecules, split valence basis set can be used to reduce the CPU time required for the calculation. The good example of split–valence basis sets are 3–21G and 6–31G basis set, it comprises of 6 gaussians for inner–shell orbital, 3 gaussians for the first STO of valence orbital and 1 gaussian for the second STO.

1.2.3.3 Polarized functions

Polarization functions are basis functions with angular momenta higher than those occupied in an atomic self–consistent field calculation. This function change the shape of the atomic orbitals from that adopted in the atom to account for a shift of the center gravity of the charge density from the atomic nucleus. Polarization functions have their radial maximum in the same region as the valence orbitals. The polarized basis sets for these function has been detailed in to basic set such as 6–31G(d).

1.2.3.4 Diffused functions

Basis sets with additional diffuse functions are large by size versions of s– and p–type split valence basis sets. Diffuse orbitals occupy a larger region of space. The effect of adding diffuse functions is usually to change the relative energies of the various geometries associated with these systems. An example for diffuse basis function is the 6–31+G(d, p) basis set [19].

1.2.3.5 Effective core potentials

Orbitals of core electron require a large number of basis function to provide an accuracy description [18]. This normally applies to third and higher row elements. Effective core potentials (ECPs) are used to replace the inner (core) electrons of atomic and molecular systems by an effective potential and treat only the valence electrons explicitly in quantum mechanical calculations.

1.2.4 NBO analysis

The NBO analysis relates to the sequential transformation of non–orthogonal atomic orbitals (AOs) to the complete and orthonormal sets of "natural" atomic orbitals (NAOs), hybrid orbitals (NHOs), and bond orbital (NBOs) [19]. These localized basis sets describe electron density and other properties by the smallest number of filled orbitals in the most rapidly convergent system. These orbital are closely related to the localized orbitals (bonds and lone pairs) used by organic chemists. The NBO method was developed by Weinhold and co-authors and it is becoming a powerful and popular method for study of bonding concepts.

1.2.5 The density of state (DOS)

DOS is essentially the number of different states at a particular energy level that electrons are allowed to occupy, such as the number of electron states per unit. DOS calculations allow to determine the general distribution of states as a function of energy and can also determine the energy gap [19].

1.2.6 Thermodynamic properties

The basic equations used to describe thermochemical quantities such as enthalpy, free energy and rate of reaction [26].

1.2.6.1 Enthalpies and Gibbs free energies of reaction

Enthalpies can be calculated by the different sum of heat of transform of the reaction using equations as follow:

$$\Delta_r H^\circ(298K) = \sum_{prod} \Delta_f H^\circ_{prod}(298K) - \sum_{react} \Delta_f H^\circ_{react}(298K) \tag{1.22}$$

Nevertheless, Gaussian program provides the short cut to calculate the enthalpy of reaction is defined as

$$\Delta_r H^\circ(298K) = \sum_{prod} \left(\varepsilon_0 + H_{corr}\right)_{prod} - \sum_{react} \left(\varepsilon_0 + H_{corr}\right)_{react} \tag{1.23}$$

where ε_0 for the total electronic energy. H_{corr} is correction to the enthalpy due to internal energy which can be calculated by

$$H_{corr} = E_{tot} + k_B T \tag{1.24}$$

where E_{tot} (total internal energy) is the sum of E_t, E_r, E_v, E_e (internal energy due to translation, rotational, vibrational and electronic motion, respectively).

$$E_{total} = E_t + E_r + E_v + E_e \tag{1.25}$$

Similarly to the enthalpies, Gibbs free energies of reaction can be calculated by the same short cut:

$$\Delta_r G^\circ(298K) = \sum_{prod} \left(\varepsilon_0 + G_{corr}\right)_{prod} - \sum_{react} \left(\varepsilon_0 + G_{corr}\right)_{react} \tag{1.26}$$

Where the correction to the Gibbs free energy due to internal energy (G_{corr}) can be calculated by

$$G_{corr} = H_{corr} - TS_{tot} \tag{1.27}$$

$$S_{tot} = S_t + S_r + S_v + S_e \tag{1.28}$$

where S_{tot} (total internal entropy) is the sum of S_t, S_r, S_v, S_e (entropy due to translation, rotational, vibrational and electronic motion, respectively).

1.2.6.2 Rate of reaction

The rate of reaction $(k(T))$ is defined by equation:

$$k(T) = \kappa \, \frac{k_B T}{h} \frac{Q_{TS}}{Q_{REA}} \exp\left(\frac{-\Delta^{\ddagger}E}{RT}\right) \tag{1.29}$$

where k_B is the Boltzmann's constant, T is the absolute temperature h is Plank's constant, and R is the gas constant. $\Delta^{\ddagger}E$ is activation energy of the reaction. Q_{TS} and Q_{REA} are the partition functions of the transition state and reactant respectively. When Q_{total} is sum of the partition function of translational, rotational, vibrational and electronic energy states.

$$Q_{total} = Q_{trans} + Q_{rotational} + Q_{vibration} + Q_{electric} \tag{1.30}$$

1.3 Objective

In this study, the adsorption of diatomic gases (H_2, N_2, O_2, CO, NO), triatomic gases (CO_2, N_2O, NO_2, H_2O, SO_2), tetratomic gas (NH_3) on the BeOSL cage and the oxidative process of CO to CO_2 on the BeOSL surface with NO_2 gas have been reported. The thermodynamic and electronic properties have been investigated using DFT method.

CHAPTER II

COMPUTATIONAL DETAILS

2.1 Structure optimization

Full optimizations of the BeOSL cluster ($Be_{12}O_{12}$) and its adsorption configurations with diatomic gases (H_2, N_2, O_2, CO, NO), triatomic gases (CO_2, N_2O, NO_2, H_2O, SO_2), tetratomic gas (NH_3) were carried out using density functional theory (DFT) method. The DFT calculations were performed with the Becke's three−parameter exchange functional with the Lee–Yang–Parr correlation functional (B3LYP) [27–28]. Geometry optimizations of all studied compounds were carried out using DFT method at the B3LYP/6–31+G(d,p) level of theory. There are two different active sites of the BeOSL namely Be and O atoms. Thermodynamic quantities of adsorption were derived from frequencies calculations of corresponding adsorption structures at the same level of theory. The transition state (TS) for of studied reaction was located using TS keyword implemented in the GAUSSIAN 09 program [29]. The TS was confirmed by intrinsic reaction coordinates (IRC) calculations to verify that each saddle point links desired minima. All calculations were performed with the GAUSSIAN 09 program.

2.2 Definitions of reaction terms

2.2.1 Adsorption of small gases on beryllium oxide

The adsorption energy (ΔE_{ads}) for gas molecules adsorbed on the beryllium oxide has been computed by the equation

$$\Delta E_{ads} = E_{G/BeOSL} - \left(E_{BeOSL} + E_G \right) \tag{2.1}$$

where $E_{G/BeOSL}$ is the total energy of gas adsorbed on BeOSL, E_{BeOSL} is the total energy of isolated BeOSL and E_G is total energy of free gas molecule.

2.2.2 Thermodynamic quantities

The standard enthalpy ΔH_{298} and Gibbs free energy changes ΔG_{298} of adsorption of small gases molecule onto BeOSL have been derived from the frequency calculations at the same level of theory. The equilibrium constant (K) was computed using equation (2.2).

$$K = e^{\frac{-\Delta G_{298}}{RT}} \tag{2.2}$$

2.2.3 Kinetic terms

Rate constant (k) of reaction step via corresponding transition state was computed by following equations.

$$k(T) = \kappa A \exp\left(\frac{-\Delta^{\ddagger}E}{RT}\right) = \kappa \frac{k_B T}{h} \frac{Q_{TS}}{Q_{REA}} \exp\left(\frac{-\Delta^{\ddagger}E}{RT}\right) \tag{2.3}$$

Form the equation (2.3) we can conclude that A, a pre–exponential factors can be rearrange into

$$A = \frac{k_B T}{h} \frac{Q_{TS}}{Q_{REA}} \tag{2.4}$$

The kappa constant κ can be calculated by equation (2.5)

$$\kappa = 1 + \frac{1}{24}\left(\frac{h\nu_i}{k_B T}\right)^2 \tag{2.5}$$

when ν_i is the imaginary frequency in the transition state of reactant molecule dissociation when it crosses the barrier. All of parameters such as activation energy, partition function of transition state and reactant were obtained from output files generated by the GAUSSIAN 09 program.

CHAPTER III

RESULTS AND DISCUSSIONS

Adsorptions of diatomic gases (H_2, N_2, O_2, CO, NO), triatomic gases (CO_2, N_2O, NO_2, H_2O, SO_2) and tetratomic gas (NH_3) on the BeOSL and the oxidative process of CO to CO_2 on the BeOSL surface with NO_2 have been studied. Adsorption energies of all studied gases on the BeOSL and their thermodynamic and electronic properties have been obtained.

3.1 The structure of BeOSL

The B3LYP/6–31+G(d,p)–optimized structure of the BeOSL obtained by full geometry optimization is shown in Figure 3.1. As the BeOSL structure is composed of hexagonal and tetragonal faces, two different B–O bonds of which the lengths are 1.52 and 1.58 Å. Bond angle between O1–Be1–O3 is 98.13º while the O2–Be1–O3 is 124.70º.
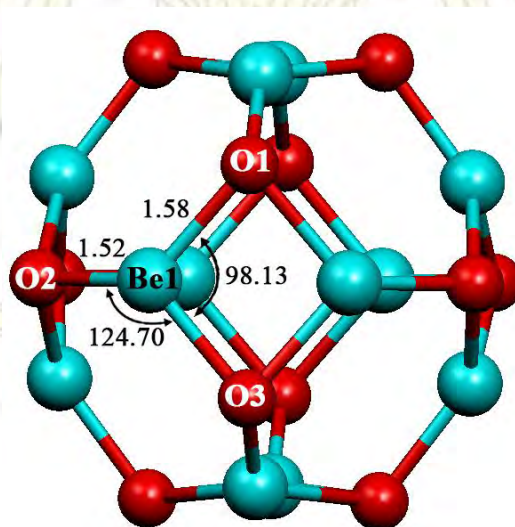
Figure 3.1 The B3LYP/6–31+G(d,p)–optimized structure of the BeOSL

Table 3.1 The selected geometrical parameters for the BeOSL cage, computed at the
B3LYP/6–31+G(d,p) level of theory.

Parameters [a]	B3LYP/6–31+G(d,p)
Bond lengths: [b]	
Be1–O1, Be1–O3,	1.58
Be1–O2	1.52
Bond angle: [c]	
O1–Be1–O3	98.13
O2–Be1–O3	124.70
Dihedral angle: [c]	
O2–Be1–O3–Zn2	133.30
O2–Be1–O3–Zn3	22.23
Be1–O3–Be3–O4	−21.95

[a] Labeling of atoms is shown in Figure 3.1.

[b] In Å.

[c] In degrees.

3.2 Adsorption structures of gases on the BeOSL cluster

3.2.1 Adsorption of gases on the BeOSL

The B3LYP/6–31+G(d,p)–optimized structures of adsorption configurations of diatomic gases (H_2, N_2, O_2, CO, NO), triatomic gases (CO_2, N_2O, NO_2, H_2O, SO_2) and tetratomic gases (NH_3) on the BeOSL are shown in Figure 3.2 and 3.3 respectively. There are two adsorption configurations for CO (C$\underline{O}$/BeOSL and $\underline{C}$O/BeOSL), NO (N$\underline{O}$/BeOSL and $\underline{N}$O/BeOSL) and N_2O ($N_2\underline{O}$/BeOSL and $\underline{N}_2$O/BeOSL) adsorbed on the BeOSL cage; underlined atomic symbol is defined as gas atom pointing toward the surface atom. Alignment of all diatomic gases except NO and O_2 are pointing their atom–end toward Be atom in the BeOSL cage. N1–O4 bonds of N$\underline{O}$ (point oxygen atom toward surface atom) and $\underline{N}$O (point nitrogen atom toward surface atom) molecules align parallel to the Be–O1 bond of the BeOSL while O4–O5 bond of O_2 molecule aligns parallel to the Be–O1 bond. For triatomic gases, N_2O and NO_2 point their atom–end toward Be atom of the BeOSL but S1–O4 bond of SO_2 molecule aligns parallel to Be–O1 bond. For CO_2 molecule, its oxygen atom points approximately perpendicular to Be–O3 bond. The adsorption structure of NH_3 on the BeOSL has quite similar structure to H_2O but points its H2–O4 bond perpendicular O4–Be bond.

Adsorption abilities of the BeOSL with studied gases shown in Table 3.2 are in orders: O_2 ($\Delta E_{ads} = -4.47$ kcal/mol) > $\underline{C}$O ($\Delta E_{ads} = -3.29$ kcal/mol) > N$\underline{O}$ ($\Delta E_{ads} = -2.33$ kcal/mol) > N_2 ($\Delta E_{ads} = -1.48$ kcal/mol) > N$\underline{O}$ ($\Delta E_{ads} = -1.19$ kcal/mol) > C$\underline{O}$ ($\Delta E_{ads} = -1.15$ kcal/mol) > H_2 ($\Delta E_{ads} = -0.19$ kcal/mol) for diatomic gases, NO_2 ($\Delta E_{ads} = -39.54$ kcal/mol) > NH_3 ($\Delta E_{ads} = -13.91$ kcal/mol) > H_2O ($\Delta E_{ads} = -9.65$ kcal/mol) > SO_2 ($\Delta E_{ads} = -4.92$ kcal/mol), > $N_2\underline{O}$ ($\Delta E_{ads} = -3.1$ kcal/mol) > CO_2 ($\Delta E_{ads} = -2.71$ kcal/mol), $\underline{N}_2$O ($\Delta E_{ads} = -2.1$ kcal/mol) for triatomic and tetratomic gases. Density of states (DOS plot) can indicated the energy gap of the molecule which can see from graph besides the adsorbed molecules.

3.2.2 NBO charges of all structures

Natural bond orbital (NBO) in Table 3.3 revealed that charges on the Be adsorption site of the BeOSL cage are within 1.49 to 1.262 e. Charge change (ΔQ) on the Be adsorption site are all in negative quantities except H_2/BeOSL. Negative quantities for charge change imply that all gas molecules, except H_2 transfer their electron to Be adsorption site.

3.2.3 Frontier orbitals and energy gap

Energies of frontier orbitals and energy gaps of the BeOSL and its adsorption complexes are shown in Table 3.4. The changes of energy gaps of all adsorption complexes compared with clean BeOSL are -72, -60, -51, -33% for adsorptions of O_2, NO, SO_2 and NO_2, respectively. Results may suggest that the BeOSL cage can be used for detection of oxygen and/or nitric oxide.
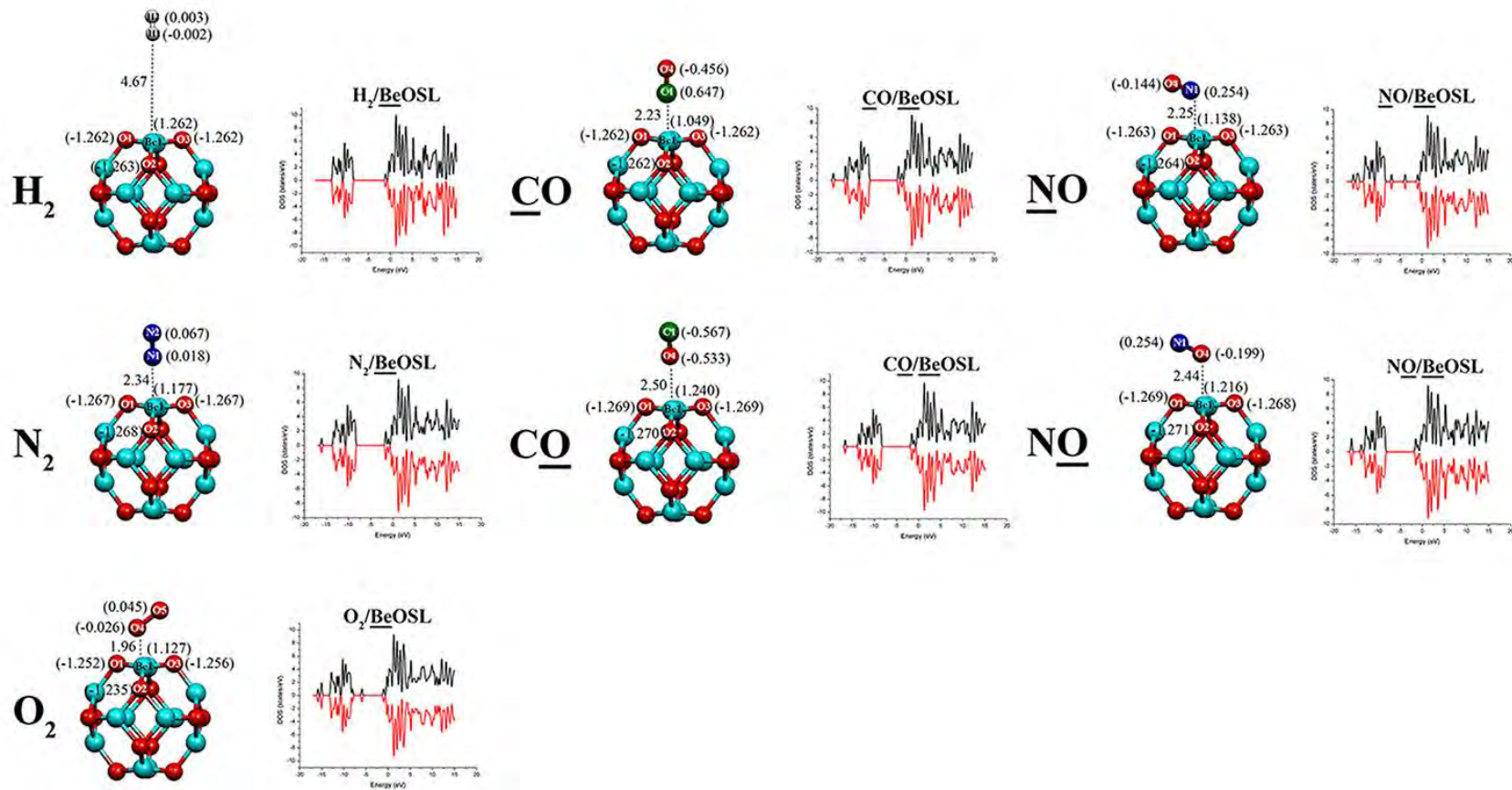
Figure 3.2. The B3LYP/6−31+G(d,p)–optimized structures of diatomic gases on the BeOSL cage, as adsorption with (a) H_2, (b) N_2, (c) O_2, (d) CO (its C toward Be atom), (e) CO (its O toward Be atom), (f) NO (its N toward Be atom) and (g) NO (its O toward Be atom). Their DOS plots are beside. Bond distances are in Å.
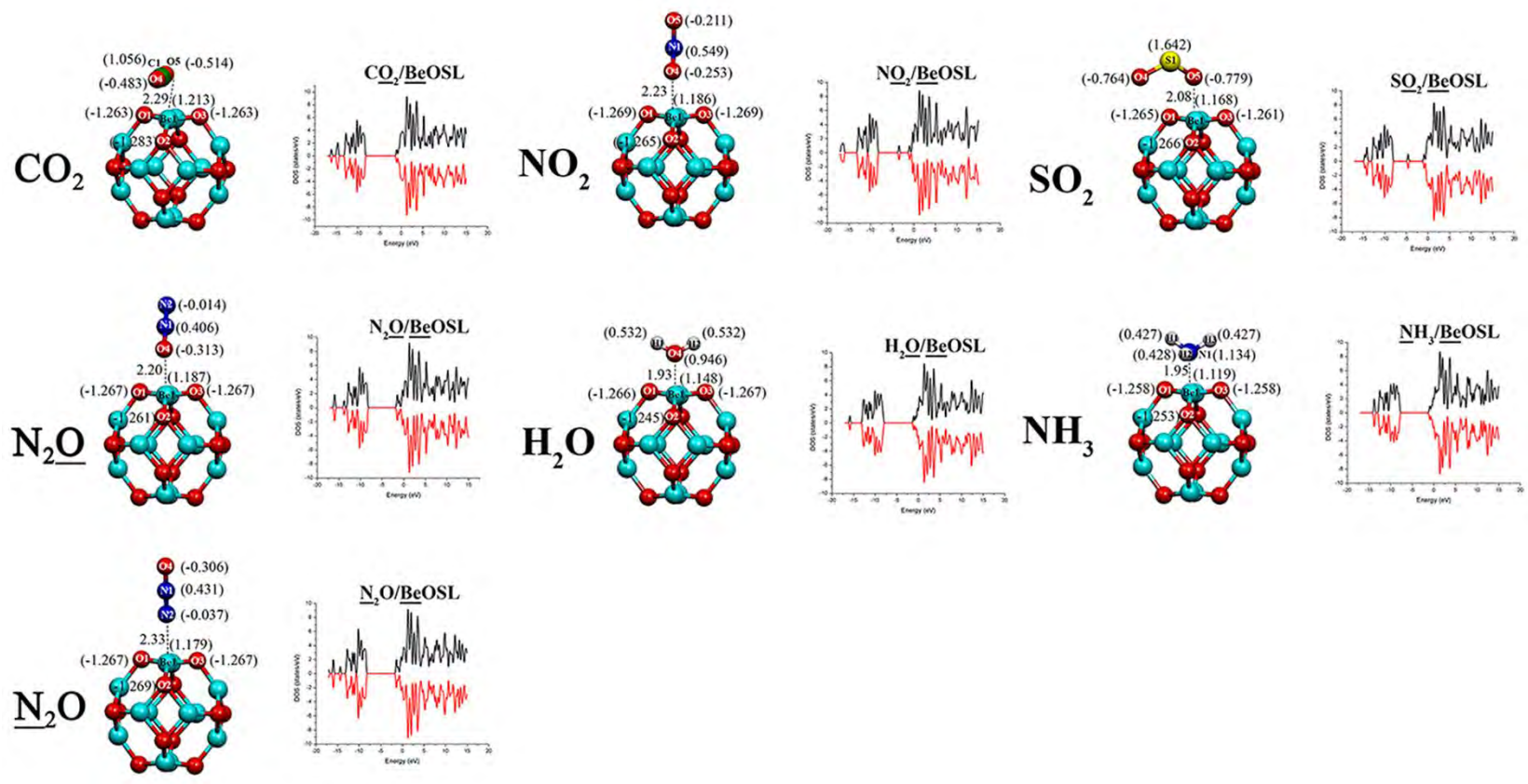
Figure 3.3. The B3LYP/6−31+G(d,p) −optimized structures of tri− and tetra−atomic gases on the BeOSL cage, as adsorption with (a) CO_2, (b) N_2O (its O toward Be atom), (c) N_2O (its N toward Be atom), (d) N_2O, (e) H_2O, (f) SO_2 and (g) NH_3. Their DOS plots are beside. Bond distances are in Å.

Table 3.2 Adsorption energies of diatomic, triatomic and tetratomic gases on the BeOSL cage, computed at the B3LYP/6−31+G(d,p) level of theory.

Gases adsorption			Adsorption		
			ΔE_{ads} [a]	ΔH^o_{298} [a]	ΔG^o_{298} [a]
Diatomic					
BeOSL + H_2	$\rightarrow$	H_2/BeOSL	−0.19	−1.10	3.37
BeOSL + N_2	$\rightarrow$	N_2/BeOSL	−1.48	−1.12	5.78
BeOSL + O_2	$\rightarrow$	O_2/BeOSL	−4.47	−4.28	3.91
BeOSL + CO	$\rightarrow$	$\underline{C}$O/BeOSL	−3.29	−3.14	4.96
BeOSL + CO	$\rightarrow$	C$\underline{O}$/BeOSL	−1.15	−0.59	5.53
BeOSL + NO	$\rightarrow$	$\underline{N}$O/BeOSL	−2.33	−1.89	5.31
BeOSL + NO	$\rightarrow$	N$\underline{O}$/BeOSL	−1.19	−0.66	5.85
Triatomic					
BeOSL + CO_2	$\rightarrow$	CO_2/BeOSL	−2.71	−2.20	5.01
BeOSL + N_2O	$\rightarrow$	$\underline{N}_2O$/BeOSL	−2.01	−2.61	5.53
BeOSL + N_2O	$\rightarrow$	$N_2\underline{O}$/BeOSL	−3.01	−1.45	5.43
BeOSL + NO_2	$\rightarrow$	$\underline{N}O_2$/BeOSL	−39.54	−38.72	−31.52
BeOSL + H_2O	$\rightarrow$	H_2O/BeOSL	−9.65	−10.06	−0.67
BeOSL + SO_2	$\rightarrow$	SO_2/BeOSL	−4.92	−2.20	5.01
Tetratomic					
BeOSL + NH_3	$\rightarrow$	NH_3/BeOSL	−13.91	−14.29	−5.03

[a] In kcal/mol.

Table 3.3 Selected NBO charges (in electrons) of the BeOSL and adsorbed gases, computed at the B3LYP/6−31+G(d,p) level of theory.

Adsorption structure	Partial charge [a]								ΔQ (Be)[b]
	BeOSL atoms				Gas atoms				
	O1	O2	O3	Be	1st	2nd	3rd	4th	
BeOSL	−1.262	−1.262	−1.262	1.262	–	–	–	–	–
H₂:					**H1**	**H2**			
H₂/BeOSL	−1.262	−1.263	−1.262	1.262	−0.002	0.003	–	–	0.000
N₂:					**N1**	**N2**			
N₂/BeOSL	−1.267	−1.268	−1.267	1.177	0.067	0.018	–	–	−0.085
O₂:					**O4**	**O5**			
O₂/BeOSL	−1.252	−1.235	−1.256	1.127	−0.026	0.045	–	–	−0.135
CO:					**C1**	**O4**			
CO/BeOSL	−1.262	−1.262	−1.262	1.049	0.647	−0.456	–	–	−0.213
OC/BeOSL	−1.269	−1.270	−1.269	1.240	−0.567	−0.533	–	–	−0.022
NO:					**N1**	**O4**			
NO/BeOSL	−1.263	−1.264	−1.263	1.138	0.254	−0.144	–	–	−0.124
ON/BeOSL	−1.269	−1.271	−1.268	1.216	0.254	−0.199	–	–	−0.046
H₂O:					**H1**	**H2**	**O4**		
H₂O/BeOSL	−1.266	−1.245	−1.267	1.148	0.532	0.532	−0.946	–	−0.114
N₂O:					**N1**	**N2**	**O4**		
ON₂/BeOSL	−1.267	−1.261	−1.267	1.187	0.406	−0.014	−0.313	–	−0.075
N₂O/BeOSL	−1.267	−1.269	−1.267	1.179	0.431	−0.037	−0.306	–	−0.083
NO₂:					**N1**	**O4**	**N5**		
NO₂/BeOSL	−1.269	−1.265	−1.269	1.186	0.549	−0.253	−0.211	–	−0.076
CO₂:					**C1**	**O4**	**O5**		
CO₂/BeOSL	−1.263	−1.283	−1.263	1.213	1.056	−0.483	−0.514	–	−0.049
SO₂:					**S1**	**O4**	**O5**		
SO₂/BeOSL	−1.265	−1.266	−1.261	1.168	1.642	−0.764	−0.779	–	−0.094
NH₃:					**N1**	**H1**	**H2**	**H3**	
NH₃/BeOSL	−1.258	−1.253	−1.258	1.119	−1.134	0.427	0.428	0.427	−0.143

[a] In e.

[b] partial charge for Be atom of the BeOSL

Table 3.4 Energies of frontier orbitals and energy gap of the BeOSL cage and its adsorption complexes, computed at the B3LYP/6−31+G(d,p) level of theory.

Compound	E_{HOMO}[a]	E_{LUMO}[a]	E_g[a,b]	ΔE_g[c]
BeOSL	−8.56	−1.05	7.51	−
Diatomic				
H_2/BeOSL	−8.56	−1.05	7.51	0.00
N_2/BeOSL	−8.46	−1.57	6.89	−8.26
O_2/BeOSL	−7.96	−5.85	2.12	−71.77
$\underline{C}O$/BeOSL	−8.42	−1.69	6.73	−10.39
$C\underline{O}$/BeOSL	−8.48	−1.50	6.98	−7.60
$\underline{N}O$/BeOSL	−6.82	−3.75	3.07	−59.12
$N\underline{O}$/BeOSL	−6.65	−3.65	3.00	−60.50
Triatomic				
CO_2/BeOSL	−8.44	−1.05	7.39	−1.60
$\underline{N}_2O$/BeOSL	−8.42	−1.37	6.90	−8.12
$N_2\underline{O}$/BeOSL	−8.41	−1.51	7.05	−6.13
$\underline{N}O_2$/BeOSL	−8.42	−3.38	5.04	−32.89
H_2O/BeOSL	−8.12	−1.07	7.06	−6.00
SO_2/BeOSL	−8.23	−4.54	3.68	−51.00
Tetratomic				
NH_3/BeOSL	−7.93	−0.93	7.00	−6.80

[a] In eV.

[b] Defined as $E_{LUMO}−E_{HOMO}$.

[c] Defined as change of energy gap of gas–adsorption complex compared with clean BeOSL cage (E_g= 7.51 eV), in percentage.

3.3 Oxidation of CO to CO$_2$ on the BeOSL surface by N$_2$O

The oxidative reaction of CO by N$_2$O on the BeOSL producing non–toxic gas N$_2$ and CO$_2$, is shown as following question:

$$BeOSL + CO + N_2O \longrightarrow BeOSL + N_2 + CO_2 \qquad (3.1)$$

The overall reaction is composed of five elementary steps, as shown in Table 3.5. Structures of all compounds involved with the oxidation are shown in Figure 3.4. Due to gases adsorption on BeOSL listed in Table 3.2, adsorption energies of CO ($\Delta E_{ads} = -3.29$ kcal/mol) is slightly stronger than that of N$_2$O ($\Delta E_{ads} = -3.1$ kcal/mol). The pre–adsorption of CO on the BeOSL (denoted by CO/BeOSL) was firstly introduced and the N$_2$O adsorption on the CO/BeOSL was taken place. The first and second steps are therefore the adsorption of CO and co–adsorption of N$_2$O, respectively. The next reaction step is the conversion step to result the co–adsorption of CO$_2$ and N$_2$ on the BeOSL via transition state TS1, as shown in Figure 3.5. Due to the TS1, the activation energy of 46.14 kcal/mol was accordingly obtained. The last step is desorption of N$_2$ and CO$_2$ from the BeOSL. The overall reaction is exothermic process with 83.76 kcal/mol. Based on the rate determining step (the third step), rate constant of 3.34×10^{-22} s^{-1} was obtained. Gibbs free energy of the reaction indicated that the oxidation reaction of CO to CO$_2$ with N$_2$O on the BeOSL cage is non–spontaneous at 298 K.
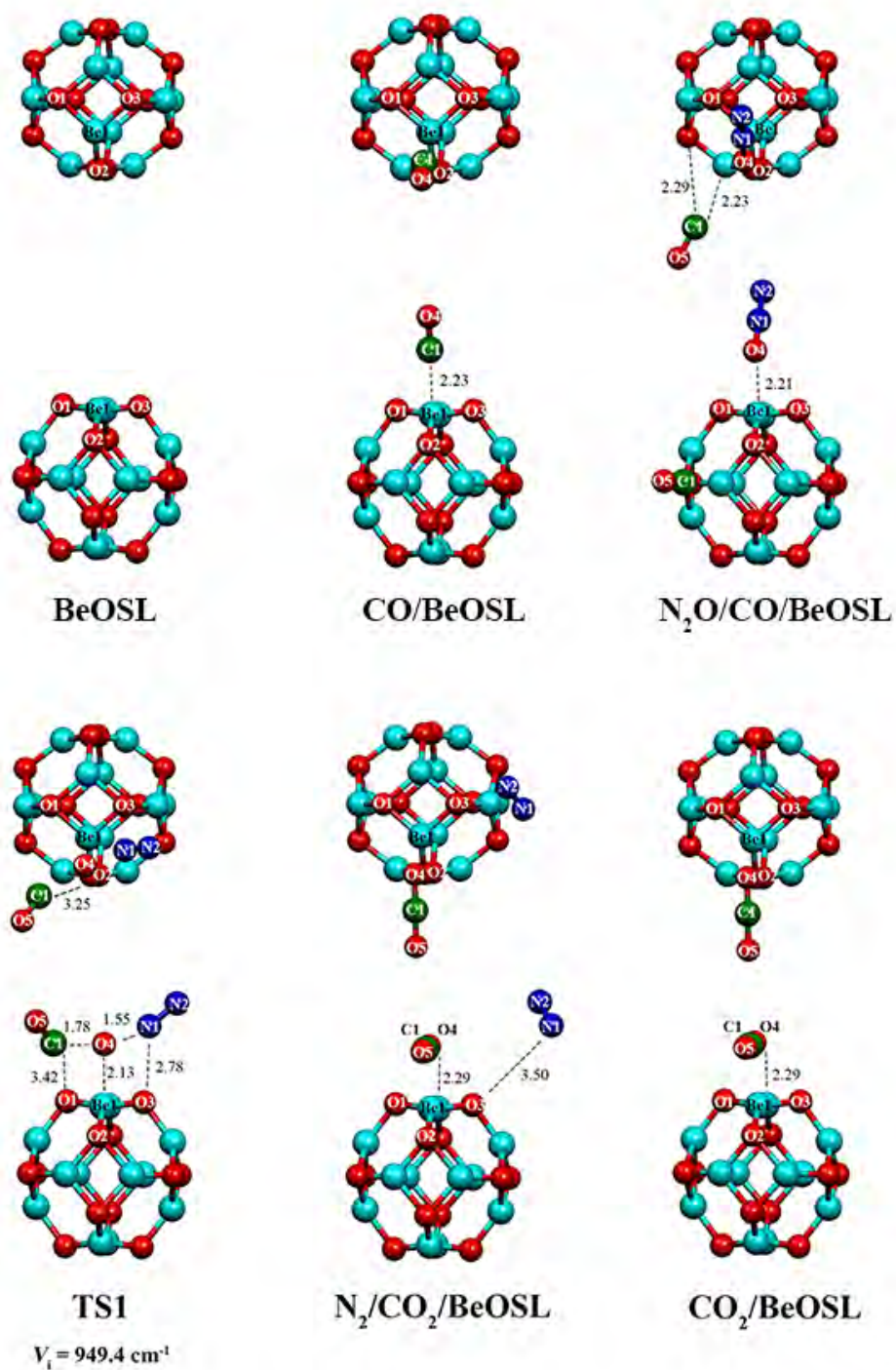
Figure 3.4 B3LYP/6−31+G(d,p)–optimized structures of the BeOSL, its top and bottom are top and side views, respectively. Adsorption and transition states bond distances are in Å.

Table 3.5 Energetics, thermodynamic properties, rate constants, and equilibrium constants of CO oxidation to CO_2 on the BeOSL by N_2O, computed at the B3LYP/6−31+G(d,p) level of theory.

Reaction	$\Delta E^{\ddagger\,a}$	$\Delta G^{\ddagger\,a}$	$k_{298}{}^b$	ΔE^a	$\Delta H_{298}{}^a$	$\Delta G_{298}{}^a$	K_{298}
Adsorption step:							
BeOSL + CO → CO/BeOSL	−	−	−	−3.29	−3.14	4.96	2.30x10^{-4}
N_2O + CO/BeOSL → N_2O/CO/BeOSL	−	−	−	−2.84	−2.91	6.86	9.32x10^{-6}
Conversion step:							
N_2O/CO/BeOSL → TS → N_2/CO_2/BeOSL	46.14	45.84	3.34×10^{-22}	−80.78	−80.24	−84.43	7.82x10^{61}
Desorption step:							
N_2/CO_2/BeOSL → N_2 + CO_2/BeOSL	−	−	−	0.44	0.29	−5.33	8.3x10^{3}
N_2 + CO_2/BeOSL → N_2 + CO_2 + BeOSL	−	−	−	2.71	2.20	−5.01	4.68x10^{3}

[a] In kcal/mol.

[b] In s^{-1}.
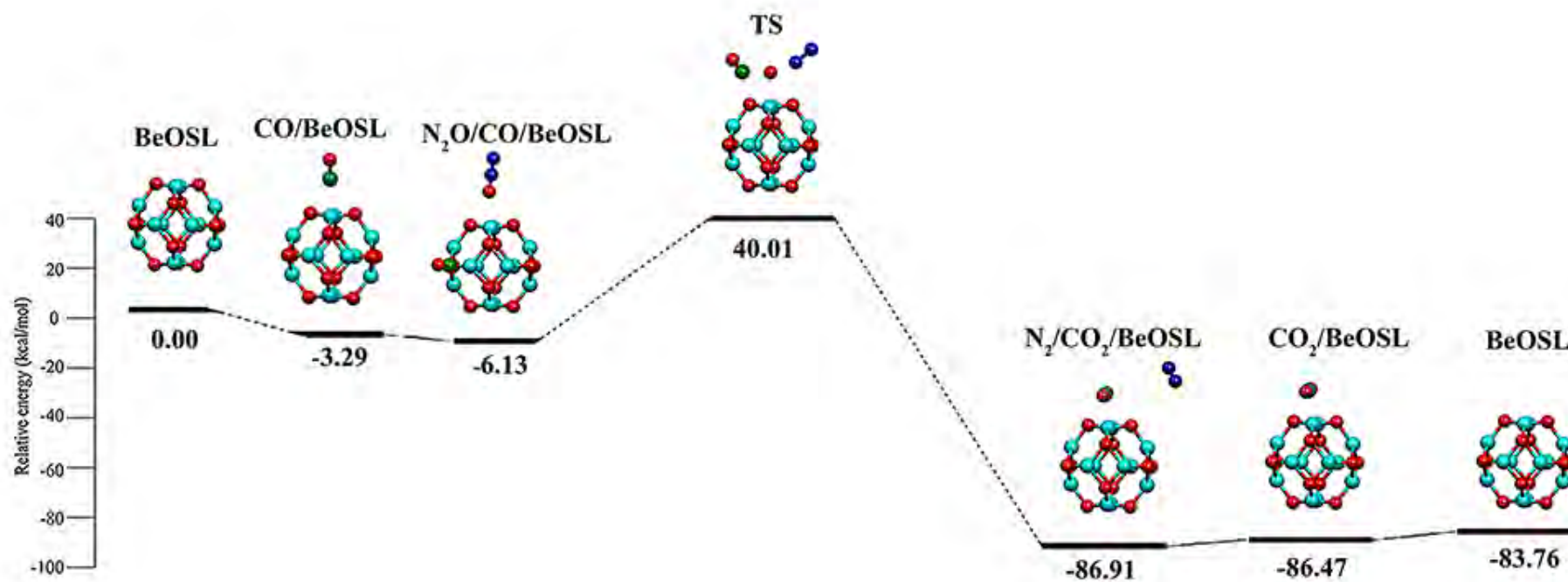
Figure 3.5. Potential energy profile for CO conversion to CO_2 on the BeOSL surface by N_2O.

CHAPTER IV

CONCLUSIONS

The adsorptions of diatomic, triatomic and tetratomic gases on the BeOSL for all possible configurations were calculated using the B3LYP/6−31+G(d,p) method. All the results can be concluded as follows:

- The adsorptions of small molecule gases on the BeOSL are physical adsorption
- The energy gaps of the BeOSL are remarkably reduced after adsorptions of O_2 and NO.
- NO_2 adsorbed on BeOSL is strongest adsorption with −39.54 kcal/mol
- Suggest that the BeOSL cluster can be used as the sensing material for NO_2 and O_2

The BeOSL cage can be used as catalyst in oxidation of CO by N_2O to afford CO_2 and N_2 of which reaction mechanism is composed of five steps. The overall reaction was found to be the energetic preferred process and non–spontaneous at 298 K as suggested by the Gibbs free energy.

REFERENCES

[1] Kim, S. K.; Ko, W. I.; Kim, H. D.; Revankar, S. T.; Zhou, W.; Jo, D., Cost-benefit analysis of BeO-UO$_2$ nuclear fuel. *Progress in Nuclear Energy* **2010,** *52* (8), 813-821.

[2] Shinde, R.; Tayade, M., Remarkable hydrogen storage on beryllium oxide clusters: First-principles calculations. *Journal of Physical Chemistry C* **2014,** *118* (31), 17200-17204.

[3] Bashiri, H.; Eris, S., Statistical Thermodynamic Study of Gas Adsorption with Different Adsorption Geometries on Homogeneous Solid Surface. *Chemical Engineering Communications* **2016,** *203* (5), 628-634.

[4] Nekooghadirli, R.; Taghizadeh, M.; Mahmoudi Alami, F., Adsorption of Pb(II) and Ni(II) From Aqueous Solution by a High-Capacity Industrial Sewage Sludge-Based Adsorbent. *Journal of Dispersion Science and Technology* **2016,** *37* (6), 786-798.

[5] Xu, H.; Qu, Z.; Zong, C.; Quan, F.; Mei, J.; Yan, N., Catalytic oxidation and adsorption of Hg0 over low-temperature NH$_3$-SCR LaMnO$_3$ perovskite oxide from flue gas. *Applied Catalysis B: Environmental* **2016,** *186*, 30-40.

[6] Zhang, L.; Yang, W.; Wu, X. Y.; Huo, M.; Lu, C. Z.; Chen, W. Z., A polyhedron-based cobalt-organic framework for gas adsorption and separation. *Inorganic Chemistry Communications* **2016,** *67*, 10-13.

[7] Zhang, S.; Sheng, J. J.; Qiu, Z., Water adsorption on kaolinite and illite after polyamine adsorption. *Journal of Petroleum Science and Engineering* **2016,** *142*, 13-20.

[8] Zhong, D. L.; Wang, J. L.; Lu, Y. Y.; Li, Z.; Yan, J., Precombustion CO$_2$ capture using a hybrid process of adsorption and gas hydrate formation. *Energy* **2016,** *102*, 621-629.

[9] Faye, O.; Raj, A.; Mittal, V.; Beye, A. C., H$_2$S adsorption on graphene in the presence of sulfur: A density functional theory study. *Computational Materials Science* **2016,** *117*, 110-119.

[10]   Peyghan, A. A.; Yourdkhani, S., Capture of carbon dioxide by a nanosized tube of BeO: A DFT study. *Structural Chemistry* **2014,** *25* (2), 419-426

[11]   Rastegar, S. F.; Ahmadi Peyghan, A.; Soleymanabadi, H., Ab initio studies of the interaction of formaldehyde with beryllium oxide nanotube. *Physica E: Low-Dimensional Systems and Nanostructures* **2015,** *68*, 22-27.

[12]   Ahmadaghaei, N.; Noei, M., Density functional study on the sensing properties of nano-sized BeO tube toward H_2S. *Journal of the Iranian Chemical Society* **2014,** *11* (3), 725-731.

[13]   Barzilai, S.; Tavazza, F.; Levine, L. E., First-principle modeling of gold adsorption on BeO (0001). *Surface Science* **2013,** *609*, 39-43.

[14]   Noei, M.; Zare-Shahabadi, V.; Razi, S. N., Selective sensing characteristics of ca doped beo nano-sized tube toward H_2O and NH_3. *Chinese Journal of Chemical Physics* **2013,** *26* (5), 612-616.

[15]   Ma, L. C.; Zhao, H. S.; Yan, W. J., Structural, electronic and magnetic properties of linear monoatomic chains adsorption on beryllium oxide nanotube: First-principle study. *Journal of Magnetism and Magnetic Materials* **2013,** *330*, 174-180.

[16]   Ren, L.; Cheng, L.; Feng, Y.; Wang, X., Geometric and electronic structures of (BeO) N (N = 2-12, 16, 20, and 24): Rings, double rings, and cages. *Journal of Chemical Physics* **2012,** *137* (1).

[17]   Hwang, D. Y.; Mebel, A. M., Conversion of CO to formaldehyde catalyzed by BeO: A theoretical study. *Journal of Physical Chemistry A* **2001,** *105* (45), 10433-10438.

[18]   Levine, N. Quantum chemistry.6th Ed. Pearson prentice hall, **2010**.

[19]   Young, D. C. Computational chemistry, John Wiley and Sons, New York, **2001**.

[20]   Engel, T.; Reid, P. Physical chemistry. Pearson Benjamin chummings, **2009.**

[21]   Kohn, W.; Becke, A. D.; Parr, R. G., Density Functional Theory of Electronic Structure. *The Journal of Physical Chemistry* **1996,** *100* (31), 12974-12980.

[22]   Parr, R. G.; Donnelly, R. A.; Levy, M.; Palke, W. E., Electronegativity: The density functional viewpoint. *The Journal of Chemical Physics* **1978,** *68* (8), 3801-3807.

[23]   Lewars, E. Computational chemistry, Kluwer Academic Publishers, New York, **2004**.

[24]   Davidson, E. R.; Feller, D., Basis set selection for molecular calculations. *Chemical Reviews* **1986**, *86 (4)*, 681-696.

[25]   Caplin, B.R. ColesA.D. In The Electronic Structures of Solids, Academic Press: **1976**

[26]   Ochterski, J.W. Thermochemistry in Guassian. Guassian Inc., Pittsburgh **2000**.

[27]   Lee, C.; Yang, W.; Parr, R.G. *Phys. Rev. B*. **1988**, *37*, 785.

[28]   Leang, S. S.; Zahariev, F.; Gordon, M. S.; *J. Chem. Phys.* **1993**, *98*, 5648.

[29]   Frisch, M. J.; Trucks, G. W.; Schlegel, H. B.; Scuseria, G. E.; Robb, M. A.; Cheeseman, J. R.; Scalmani, G.; Barone, V.; Mennucci, B.; Petersson, G. A.; Nakatsuji, H.; Caricato, M.; Li, X.; Hratchian, H. P.; Izmaylov, A. F.; Bloino, J.; Zheng, G.; Sonnenberg, J. L.; Hada, M.; Ehara, M.; Toyota, K.; Fukuda, R.; Hasegawa, J.; Ishida, M.; Nakajima, T.; Honda, Y.; Kitao, O.; Nakai, H.; Vreven, T.; Montgomery Jr., J. A.; J. E. Peralta, J. E.; Ogliaro, F.; Bearpark, M.; Heyd, J. J.; Brothers, E.; Kudin, K. N.; Staroverov, V. N.; Keith, T.; Kobayashi, R.; Normand, J.; Raghavachari, K.; Rendell, A.; Burant, J. C.; Iyengar, S. S.; Tomasi, J.; Cossi, M.; Rega, N.; Millam, J. M.; Klene, M.; Knox, J. E.; Cross, J. B.; Bakken, V.; Adamo, C.; Jaramillo, J.; Gomperts, R.; Stratmann, R. E.; Yazyev, O.; Austin, A. J.; Cammi, R.; Pomelli, C.; Ochterski, J. W.; Martin, R. L.; Morokuma, K.; Zakrzewski, V. G.; Voth, G. A.; Salvador, P.; Dannenberg, J. J.; Dapprich, S.; Daniels, A. D.; Farkas, O.; Foresman, J. B.; Ortiz, J. V.; Cioslowski, J.; Fox, D. J. Gaussian 09, Revision B.01, Gaussian, Inc., Wallingford CT, 2010.

VITAE

Name: Pasakorn Piarabutr

Date of birth: 23th July 1992

Address: 89/16 M. ChuanChuen Chaengwattana, T. Bangpood, A. Pakret, Nonthaburi
province11120

Tel: 089-6974876   **E-mail:** zerberusohmm@gmail.com

Education: primary school at pichaya suksa school   during 2000−2005.
high school at Suankularb wittayalai Nonthaburi   during 2006−2011
Bachelor's degree of Science, Chulalongkorn University during 2012−2015.